

Stable Messenger: Steganography for Message-Concealed Image Generation

Quang Ho Nguyen^{1*} Truong Vu^{1*} Cuong Pham^{1,2} Anh Tran¹ Khoi Nguyen¹

¹VinAI Research,

²Posts & Telecommunications Inst. of Tech., Vietnam

Abstract

In the ever-expanding digital landscape, safeguarding sensitive information remains paramount. This paper delves deep into digital protection, specifically focusing on steganography. While prior research predominantly fixated on individual bit decoding, we address this limitation by introducing “message accuracy”, a novel metric evaluating the entirety of decoded messages for a more holistic evaluation. In addition, we propose an adaptive universal loss tailored to enhance message accuracy, named *Log-Sum-Exponential (LSE) loss*, thereby significantly improving the message accuracy of recent approaches. Furthermore, we also introduce a new latent-aware encoding technique in our framework named *Stable Messenger*, harnessing pre-trained *Stable Diffusion* for advanced steganographic image generation, giving rise to a better trade-off between image quality and message recovery. Throughout experimental results, we have demonstrated the superior performance of the new *LSE loss* and latent-aware encoding technique. This comprehensive approach marks a significant step in evolving evaluation metrics, refining loss functions, and innovating image concealment techniques, aiming for more robust and dependable information protection.

1. Introduction

Data hiding techniques, like watermarking and steganography, are crucial for securing sensitive information in our increasingly digital landscape. While both conceal messages within data, watermarking protects ownership, while steganography ensures secure communication. Images, with their rich presentation and widespread digital presence, serve as ideal carriers for hidden messages. Extensive research on digital image watermarking and steganography dates back to early computer vision [3, 21, 25, 27, 40]. Recent advancements in deep learning-based methods [38, 41]

*First two authors contribute equally. The work is done during Quang Nguyen’s internship at VinAI Research.

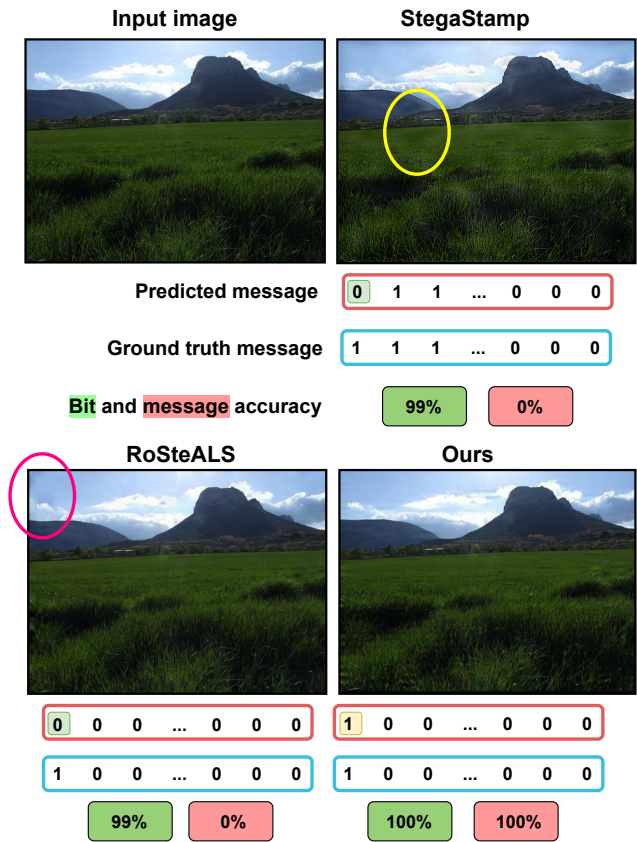


Figure 1. **Reconstructed images and messages of our method and prior work.** Although the image quality of all methods is similar, the message recovered in our approach has a much better **message accuracy** (our proposed metric) than those of prior work.

achieve highly accurate message injection and recovery while imperceptibly altering the host images. Notably, StegaStamp [35] introduces a robust steganographic approach capable of preserving hidden messages even through extreme image transformations, applicable in the real world.

In recent years, the emergence of advanced text-to-image models [1, 2, 4, 7, 28, 31, 33] has underscored the pressing need to integrate these models with data-hiding techniques.

These powerful image-generation tools provoke concerns regarding authorship protection and distinguishing between real and synthesized images. Watermarking stands out as a potential solution to address these concerns by enabling the embedding of hidden markers in synthesized images, facilitating author identification and highlighting their artificial origin. Additionally, steganography, beyond its role in secure information exchange, offers customizable watermarking to mitigate these issues. Consequently, within a remarkably short span, several papers have been published focusing on watermarking [10, 18, 22] and steganography [5] specifically tailored for text-to-image generation.

Despite the growing use of steganographic methods, previous evaluation frameworks [5, 35, 38, 41] often neglect the vital need to completely preserve hidden secrets. These studies typically rely on the bit accuracy metric, which measures individual bit decoding but fails to assess the practical utility of image watermarking and steganography. For instance, a watermarking algorithm achieving 99% bit accuracy may still fail to recover the entire message accurately, rendering it ineffective for confirming intellectual property ownership. Similarly, in steganography, even a high bit accuracy might overlook crucial errors in characters, impacting essential information like URLs, numbers, or encrypted text. Introduced alternative metrics, such as word accuracy as proposed by Bui et al. [5], fail to capture the true usability of the system. This oversight calls for a re-examination of evaluation methodologies and a redefinition of criteria to better align with real-world requirements.

To bridge this gap, we propose a novel metric, **message accuracy**, as a departure from conventional evaluation methods like bit accuracy. This new metric only considers a match when the extracted hidden message perfectly aligns with the originally embedded content, emphasizing the crucial need for preserving entire hidden information in steganographic applications. Our findings using this metric reveal that state-of-the-art steganographic models, despite near-perfect bit accuracy, often demonstrate critically low practical value. For instance, the RoSteALS system, designed for 200-bit length messages, achieves a 94% bit accuracy but rarely recovers an entirely correct message.

Moreover, conventional losses like MSE or BCE treat all predicted bits equally, which can saturate and provide uninformative guidance for network optimization when most bits are predicted correctly. To overcome this limitation, we introduce a novel loss function, the **“Log-Sum-Exponential” (LSE) loss**. Unlike MSE or BCE, LSE prioritizes the gradient based on the most wrongly predicted bits, ensuring informative guidance for network optimization even with a few incorrect predictions. This approach notably enhances results in message accuracy.

In addition, we introduce a novel technique leveraging the pre-trained Autoencoder of Stable Diffusion (SD) to em-

bed confidential messages directly into synthesized images. Our approach involves a message encoder that aligns with the image content, ensuring more compatible message encoding and enhanced concealment capabilities without additional post-steganography steps.

We evaluate our methods against established approaches, RoSteALS [5] and StegaStamp [35], for real image steganography across diverse datasets: MirFlickr [16], CLIC [23], and Metfaces [17]. Additionally, we conduct experiments in a generative setting, embedding hidden messages within newly generated images.

In summary, the contributions of our work are as follows:

1. We introduce **message accuracy**, a precise matching metric for extracted hidden messages.
2. We propose a novel **LSE loss** enhancing recovery of complete hidden messages.
3. We devise **latent-aware message encoding** using pre-trained SD for steganographic image generation.

In the following, Sec. 2 reviews prior work; Sec. 3 specifies our approaches; and Sec. 4 presents our implementation details and experimental results. Sec. 5 concludes with some remarks and discussions.

2. Related Work

A large number of techniques have been developed for image-based steganography. They can be categorized as classical, deep-learning, and generative-based methods.

Classical methods. The Least-Significant Bit (LSB) embedding method, an early hand-crafted technique [37], concealed data within the lowest bits of image pixels to create steganographic images visually akin to originals. Subsequent advancements, including spatial [11, 34] and frequency domain techniques [13, 14, 20, 26, 29, 30], aimed to increase capacity while preserving visual quality. Despite advantages, these methods rely on delicate features, making them vulnerable to even minor alterations that could lead to significant hidden information loss.

Deep-Learning-based methods. Deep learning has revolutionized steganography, enhancing accuracy, imperceptibility, and resilience. HiDDeN [41] pioneered an end-to-end framework employing an encoder-decoder architecture with a transformation layer and adversarial discriminator. Subsequent advancements in architectures [6, 8, 15, 24, 35, 38] continue to refine steganographic image quality and robustness, often emphasizing joint encoding of secrets and covers. Our approach diverges, leveraging a latent space generated by a pretrained autoencoder within Stable Diffusion, offering increased resilience to image transformations compared to direct RGB space embedding.

Generative-based methods. With advancements in text-to-image generative models like Stable Diffusion (SD) [32], new methods embedding watermarking/steganography

have emerged. Stable Signature [10] fine-tunes SD’s image decoder for steganographic image generation, but it necessitates re-finetuning for each new message. RoSteALS [5] explores VQGAN’s latent representations for concealing information but lacks image-content-aware message encoding. In contrast, our approach incorporates image latent information into the message encoder, ensuring compatibility and preserving concealed information.

Evaluation metrics for steganography. Two metric sets gauge steganography effectiveness: one assessing stealthiness through visual similarity (e.g., PSNR, SSIM, LPIPS), the other measuring reconstructed secret accuracy, commonly using bit accuracy like HiDDeN [41]. RoSteALS [5] introduces “word accuracy”, evaluating decoded messages with at least 80% bit accuracy. However, none fully assesses decoded secrets, missing watermarking and steganography practical goals. To address this, we propose “message accuracy”, evaluating entire decoded messages. Additionally, we present a novel, adaptable loss function to enhance message accuracy and bolster practical system performance.

3. Proposed Approach

Problem Statement: In steganography, user A wants to conceal a hidden message in the form of a binary string $m \in \{0, 1\}^d$ with length d within a cover image $I \in \mathbb{R}^{H \times W \times 3}$ (H and W are the image height and width) using a message encoder \mathbf{E} , ensuring that the altered image I' is visually similar to original image I . Subsequently, user B equipped with the message decoder \mathbf{D} provided by user A can extract the hidden message m' . We expect to transfer the message without any information loss, i.e., $m' = m$.

To address this problem, we make three key contributions. Firstly, we propose a strict metric known as **message accuracy**, emphasizing bit-wise identical between the extracted hidden message and the originally embedded message. Secondly, to address the strict requirements of the message accuracy metric, we introduce a novel **LSE loss** aimed at improving the recovery of the entire hidden message. Thirdly, we present a technique for **latent-aware message encoding** based on Stable Diffusion for generating steganographic images.

3.1. Message Accuracy Metric

Previous watermarking/steganography works [5, 10, 35, 38, 41] utilized *bit accuracy* computed as:

$$\text{Bit Accuracy}(m, m') = \frac{1}{d} \sum_{i=1}^d \mathbb{1}(m_i = m'_i), \quad (1)$$

where $\mathbb{1}(\cdot)$ is indicator function, and m_i, m'_i are the i -th bits of m, m' . The common practice of focusing solely on

the bit accuracy metric may inadvertently overlook the critical need for holistic message accuracy. High bit accuracy, such as achieving 99%, does not inherently guarantee the exact extraction of the entire message, as can be observed in our comparison results (Tab. 1). This oversight raises concerns about the reliability of steganographic techniques, as a seemingly high bit accuracy rate may still result in critical portions of the concealed message being inaccurately retrieved. Such a discrepancy could be especially problematic when the extracted information is used for legal or security. Thus, introducing and emphasizing the **message accuracy** metric becomes crucial and necessary for developing a reliable steganography system. A shift toward evaluating methods focusing on the comprehensive accuracy of the entire hidden message ensures a more robust and dependable assessment, aligning steganography research with real-world applicability and the stringent demands of secure information retrieval. Formally, message accuracy is calculated as:

$$\text{Message Accuracy}(m, m') = \bigwedge_{i=1}^d \mathbb{1}(m_i = m'_i), \quad (2)$$

where \wedge is the AND operator. Equivalently, a message is correct if and only if all of its bits are correct.

3.2. Loss-Sum-Exponential (LSE) Loss

To tackle the stringent requirement of the message accuracy metric, we introduce a new loss using the Log-Sum-Exponential function, named the **LSE loss**. For an input $x \in \mathbb{R}^d$, the LSE between predicted message m and ground-truth message m^* is computed as:

$$\mathcal{L}_{\text{LSE}}(m, m^*) = \log \left(\sum_{i=1}^d \exp \|m_i - m_i^*\|_2^2 \right). \quad (3)$$

Let us explain why the LSE loss helps improve message accuracy while the BCE and MSE loss functions do not. The loss of BCE or MSE becomes smaller when *most* of the bits are predicted correctly, and thus, its gradient becomes uninformative for the network’s optimization. In other words, a few bits incorrectly predicted do not affect the loss much as the loss is averaged across all bits. This is against the requirement of the message accuracy metric that all bits of the retrieved message must be correct. However, the Log-Sum-Exponential function in the LSE loss can be considered as a “soft”-max function where the maximum bit discrepancy at a position dominates the entire loss. Hence, it maintains informative gradients for updating the model’s parameters even if only a few bits are predicted wrongly.

Nevertheless, it should be cautious when using the LSE loss at the beginning of the training process. That is, when most bits are not correct, the LSE loss can “explode”. Thus, it is advised to use LSE in conjunction with BCE or MSE

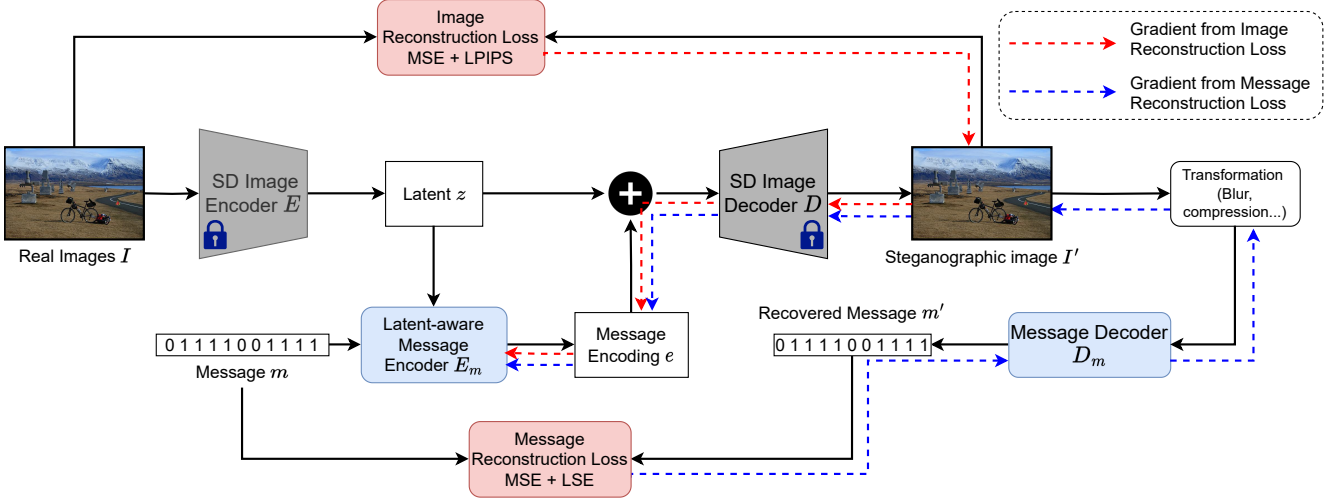


Figure 2. **Training of Stable Messenger.** Given a real image I , we utilize the Image Encoder E of SD to extract its latent z . Subsequently, the Latent-aware Message Encoder E_m takes as input the message m and latent z to produce the message encoding e . Next, the SD Image Decoder D receives the modified latent $z' = z + e$ to generate steganographic image I' . Optionally, I' can be further transformed by some operations such as blur and compress to enhance the robustness. Finally, the Message Decoder D_m recovers the hidden message m' in I' . To train the network, we use two sets of loss functions: image reconstruction and message reconstruction.

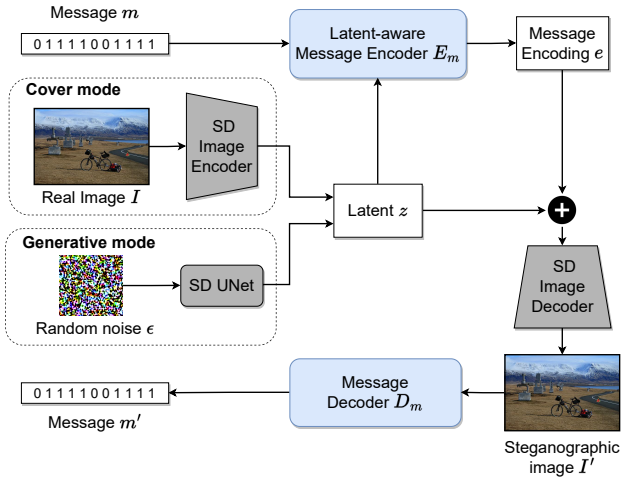


Figure 3. **Testing of Stable Messenger.** There are two modes: cover mode and generative mode. In the cover mode, the real image I is encoded into latent z with a pretrained SD Image Encoder while in the generative mode, the pretrained UNet of SD transforms a noise ϵ to latent z . Subsequent steps are similar to those in the training of Stable Messenger. See more in caption of Fig. 2.

when the model reaches a certain level of bit accuracy. It is noteworthy that the new LSE loss is applicable to various kinds of steganography approaches, not only ours.

3.3. Stable Messenger

Architecture: To begin, let us depict the training process of Stable Messenger in Fig. 2, which is based on the pretrained

Stable Diffusion [32]. First, we obtain the latent code z from the cover image I using the Image Encoder E of SD. Next, the Latent-aware message encoder E_m computes the message encoding e from the given message m and latent z , which is subsequently added to the original latent z to produce the steganographic latent $z' = e + z$. Then, the Image Decoder D of SD takes as input z' to generate the steganographic image I' . Finally, the message decoder D_m extracts the hidden message m' concealed inside I' . Note that the message encoder and decoder can be trained jointly. Optionally, steganographic image I' can be corrupted by some differentiable transformation operations, e.g., blur and compression, to enhance the robustness.

The main reason is that we want our approach to work with both **cover mode** (hide a message inside a real image) and **generative mode** (embed a message in the image generation process given a text prompt) in testing, we propose to use the image encoder and decoder of Stable Diffusion (SD) [32] as illustrated in Fig. 3. In particular, in the cover mode, the cover image can be encoded using the image encoder to a latent z while in the generative mode, the UNet of SD can be used to iteratively transform a noise $\epsilon \sim \mathcal{N}(0, I)$ to the final latent z . It is worth noting that the latent code z has the size of $\mathbb{R}^{\frac{H}{8} \times \frac{W}{8} \times 4}$ capturing the sufficient content of the image. This architecture is in contrast to prior work, RoSteALS [5] where the message encoding is created independently from the image content. In other words, the message encoder E_m is not aware of the image content so the message encoding might not be compatible with the image, resulting in information loss in the steganographic im-

Datasets	Methods	PSNR \uparrow	SSIM \uparrow	LPIPS \downarrow	Bit Acc (%) \uparrow	Message Acc (%) \uparrow
MirFlickr [16]	StegaStamp [35]	29.74	0.91	0.07	99	87
	StegaStamp [35] + LSE	29.97	0.92	0.07	99	96 (+9)
	RoSteALS [5]	33.16	0.93	0.04	99	67
	RoSteALS [5] + LSE	33.22	0.94	0.04	99	73 (+6)
	Ours	33.31	0.87	0.07	99	77
	Ours + LSE	33.11	0.87	0.07	99	94 (+17)
CLIC [23]	StegaStamp [35]	30.37	0.94	0.07	99	92
	StegaStamp [35] + LSE	30.66	0.94	0.07	99	97 (+5)
	RoSteALS [5]	33.41	0.97	0.04	99	71
	RoSteALS [5] + LSE	33.47	0.97	0.04	99	78 (+7)
	Ours	33.60	0.93	0.08	99	75
	Ours + LSE	33.27	0.93	0.08	99	95 (+20)
Metfaces [17]	StegaStamp [35]	32.04	0.95	0.12	99	96
	StegaStamp [35] + LSE	32.48	0.95	0.12	99	99 (+3)
	RoSteALS [5]	35.84	0.97	0.06	99	75
	RoSteALS [5] + LSE	35.89	0.98	0.06	99	80 (+5)
	Ours	35.29	0.92	0.11	99	91
	Ours + LSE	35.23	0.92	0.11	99	99 (+8)

Table 1. Results of our Stable Messenger and prior work with and without the LSE loss on various datasets using **100-bit message**.

age. Therefore, we propose to take the latent code z which captures the essential content of the image along with the message m as inputs to the latent-aware message encoder \mathbf{E}_m . The effectiveness of the latent-aware message encoder will be demonstrated in the Experiment section.

Training loss functions: As mentioned above, we follow two sets of training loss functions including image reconstruction and message reconstruction. For image reconstruction loss, we follow RoSteALS [5] to use LPIPS loss [39] and MSE. For the message reconstruction loss, we additionally use the LSE loss at a particular iteration t along with the MSE loss. The final loss we use to train our Stable Messenger as follows:

$$\mathcal{L} = \alpha_1 \mathcal{L}_{\text{LPIPS}}^{\text{image}} + \alpha_2 \mathcal{L}_{\text{MSE}}^{\text{image}} + \alpha_3 \mathcal{L}_{\text{LSE}}^{\text{message}} + \alpha_4 \mathcal{L}_{\text{MSE}}^{\text{message}}. \quad (4)$$

One advantage of our method is that we only train in the cover mode to speed up the training process but can test in both cover and generative modes for flexible usage.

4. Experiments

4.1. Experimental Setup

Datasets: We conduct our experiments on three datasets: MirFlickr [16], CLIC [23], and MetFaces [17]. In our experiments, we *train* on 100K real images and *validate* in two modes: cover and generative modes. For the cover mode, we tested on another set of 1,000 images of MirFlickr, 530 test images of CLIC, and 1336 test images of MetFaces.

For the generative mode, we utilize the image captions of the 1,000 images of the Flickr 8K dataset [12].

Evaluation metrics: We use two sets of evaluation metrics: image quality including PSNR [19], SSIM [36], and LPIPS [39], and message preservation encompassing Bit accuracy and Message accuracy.

Implementation details: During training, the input image is resized to 512×512 and then fed to the Image Encoder of SD [32]. We experiment with message lengths of 100 bits. We use the AdamW optimizer with a learning rate of $8e^{-5}$. By default, we set $\alpha_1 = 1.0, \alpha_2 = 1.5, \alpha_3 = 0.1, \alpha_4 = 16.0$. We also follow RoSteALS’s [5] strategy to stabilize the training. In particular, we start with a fixed image batch and then unlock the full training data after bit accuracy reaches a threshold $\tau_1 = 90\%$. After training on the full dataset and waiting for the bit accuracy to reach the threshold $\tau_2 = 95\%$, we apply image transformation to make the method more robust to the transformed inputs in testing. Empirically, we also activate the LSE loss when the bit accuracy reaches the threshold τ_2 . For the architecture of message encoder \mathbf{E}_m , first, the 1D message m is converted to a 2D message using 1 fully connected layer and subsequently concatenated with the latent z . The output is then taken as input to a UNet architecture with 4 down and 4 up layers to produce the message encoding e .

4.2. Comparison with Prior Methods

We compare our approach with the following baselines:

- RoSteALS [5]: a method uses the latent representation

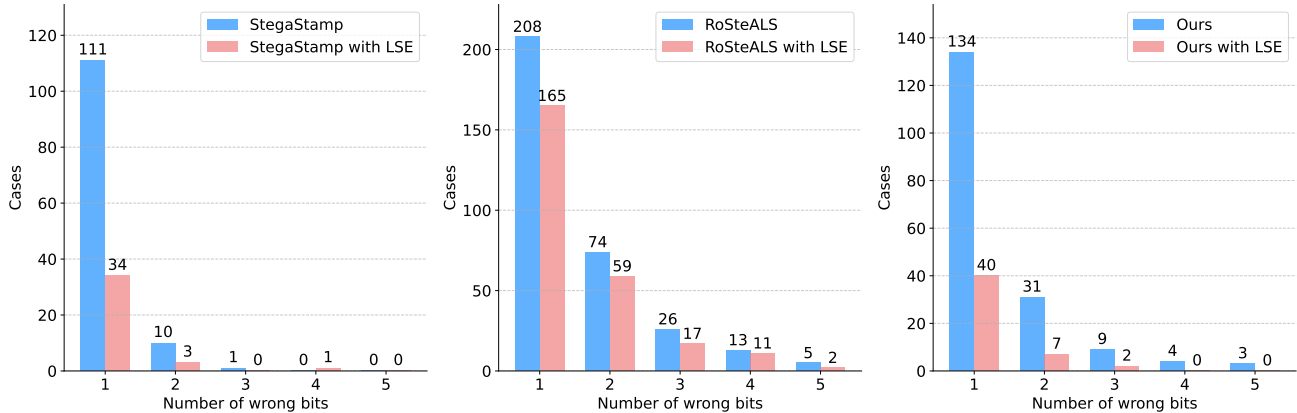


Figure 4. Histograms of wrong bits with and without using the LSE loss in StegaStamp [35], RoSteALS [5], and ours.

produced by the pretrained autoencoder of VQGAN [9] to conceal the message. We use the official code¹ to reproduce the results.

- StegaStamp [35]: a deep learning-based method. We also use the official code² to reproduce the results.

Cover mode. We present the comparative results between our approach and prior work on the three datasets MirFlickr [16], CLIC [23], and Metfaces [17] in Tab. 1. We can see that StegaStamp [35] usually has better message accuracy but lower image quality. RoSteALS [5] is a latent-based approach with higher image quality but lower message accuracy. Stable Messenger is also a latent-based approach that enjoys a better trade-off, i.e., having high image quality as RoSteALS but comparable message accuracy to StegStamp thanks to the proposed latent-aware message encoder.

Furthermore, the performance gains of using the LSE loss indicate that our LSE loss exhibits robustness across various deep-learning-based steganography methods. Applying our proposed loss consistently leads to a notable increase in message accuracy without discernible degradation in image quality. To explain why using our LSE loss helps improve the message accuracy a lot, we count the number of cases with wrong bits in each message and present them in the histogram in Fig. 4. The number of wrong bits reduced significantly after applying the LSE loss, resulting in better message accuracy.

Generative mode. In Table 2, we present a comparison between our network’s performance and RoSteALS in concealing a message during the image generation process. As RoSteALS [5] does not provide a pretrained message encoder-decoder in this mode, we had to re-implement it using the official code’s message encoder-decoder. We also retained the latent z to generate the reference image

Approach A	PSNR \uparrow	Bit Acc \uparrow	Message Acc \uparrow
RoSteALS [5]	38.90	98%	48%
Ours	35.18	99%	89%

Table 2. Results of applying steganography in the process of generating new images.

Approach B	PSNR \uparrow	SSIM \uparrow	LPIPS \downarrow	Message Acc \uparrow
RoSteALS [5]	33.79	0.96	0.04	73%
StegaStamp [35]	32.84	0.92	0.08	90%
Ours	34.37	0.90	0.04	93%

Table 3. Results of applying steganography on generated images.

for evaluating the image quality. The quantitative results demonstrate that our network is more effective than RoSteALS in recovering the hidden message, albeit at a slight cost to image quality.

Another way to apply steganography in generative mode is to apply steganography approaches to the generated images as cover images. The results in Tab. 3 suggest that our method achieves a better message accuracy, surpassing RoSteALS [5] with a gap of 20%. Compared to StegaStamp [35], we have slightly better results in message accuracy while delivering better image quality. Moreover, the question that may arise is whether to apply steganography in the process of generating images (approach A) or to generate images first and then apply steganography (approach B). Comparing the results in Tab. 2 and Tab. 3, we can conclude that when the image quality is preferable, use approach A, otherwise, use approach B.

Qualitative comparison. We present qualitative results for the cover mode in Fig. 5 and generative mode in Fig. 6. For the cover mode, each method introduces a distinct visual artifact to the cover image. For the generative mode,

¹<https://github.com/TuBui/RoSteALS>

²<https://github.com/tancik/StegaStamp>

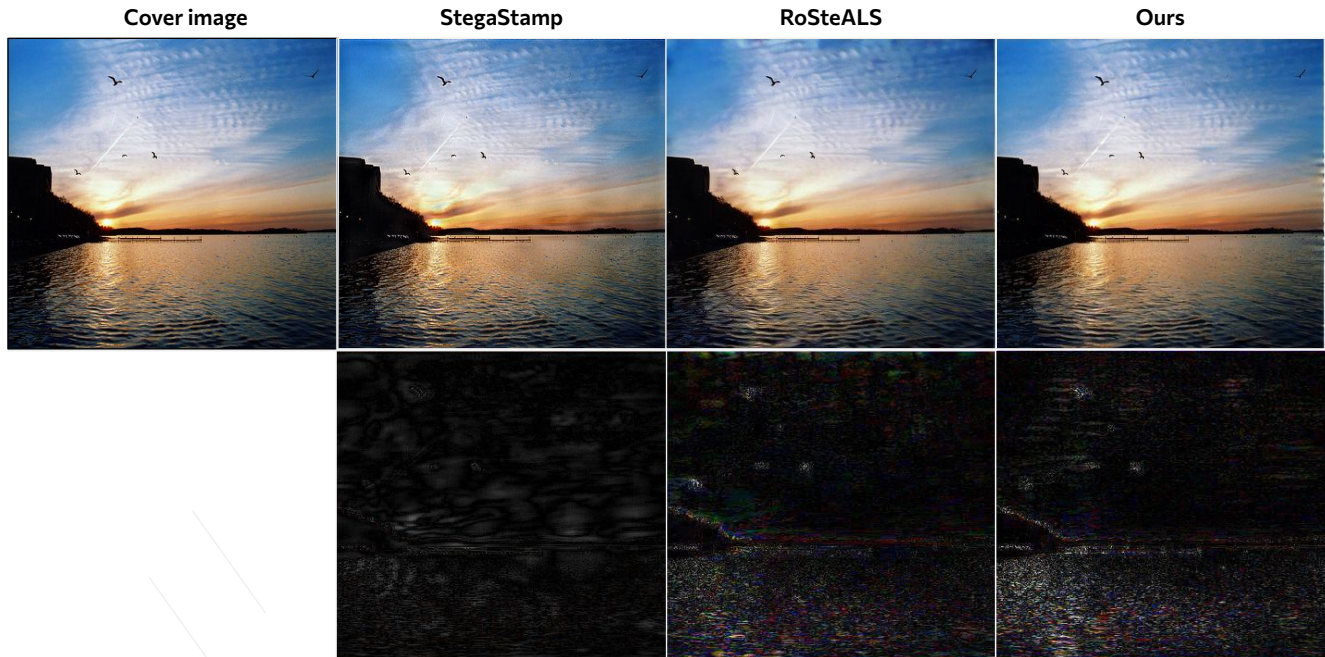


Figure 5. **Qualitative results in the cover mode.** Different methods create their artifact on the cover image. The second row shows the residual between the cover image and the steganographic image (the residual is magnified $2\times$ for visualization purposes only).



Figure 6. **Qualitative results in the generative mode.** Our method generates high-fidelity steganographic images (first three columns) but occasionally reveals hidden patterns in the resulting images (last column).

	StegaStamp [35]		RoSteALS [5]		Our + LSE	
	Bit Acc (%)	Message Acc (%)	Bit Acc (%)	Message Acc (%)	Bit Acc (%)	Message Acc (%)
No Transformation	99	87	99	67	99	94
Gaussian blur	99	89	99	61	99	94
Gaussian noise	92	1	93	2	99	46
RGB2BGR	99	86	99	53	99	92
JPEG Compression	99	85	99	60	99	93

Table 4. Robustness results on the MirFlickr [16] dataset under various color intensity transformations.

the first two columns exhibit several high-fidelity samples, while the last column showcases failure cases, where observable visual patterns emerge.

4.3. Robustness Evaluation

We aim to assess the real-world resilience of our steganographic method, comparing its performance against RoSteALS [5] and StegaStamp [35]. The experiment introduces various color intensity transformations, simulating potential modifications that steganographic images may undergo in practical scenarios. To this end, we use the provided checkpoint of RoSteALS [5], and StegaStamp [35] to compare with our proposed method. We evaluate the robustness of these steganography methods with 1000 images taken from MirFlickr [16]. Additionally, we discuss the hyper-parameters of each transformation in the supplementary document. From Tab. 4, we found that our approach is robust with several modifications such as Gaussian blur, transform color, or jpeg compression with a modest drop in message accuracy. However, the message accuracy significantly degrades if the steganographic images are injected with Gaussian noise. Nonetheless, ours still outperforms others with significant margins.

4.4. Ablation Study

Noticeably, at the beginning of the training of our approach, we only use MSE loss as our message reconstruction loss, later, after the bit accuracy reaches some threshold τ_1 , we activate the LSE loss. Thus, we study the impact of LSE coefficient α_3 and message MSE coefficient α_4 using the test set of MirFlickr [16]. Additionally, we provide more ablation studies for network design in the supplementary.

Study on LSE coefficient α_3 is shown in Tab. 5. As observed, when the coefficient is too small, it results in a low message accuracy. Our selected value of $\alpha_3 = 0.1$ yields the best results.

Study on the message MSE coefficient α_4 is shown in the Tab. 6. Our observations reveal that employing a higher value contributes to incrementally improved message accuracy with an acceptable trade-off in PSNR. Notably, it is essential to acknowledge that a higher value also accelerates the increase in bit accuracy, reaching the first threshold $\tau_1 = 90\%$ faster. Therefore, we choose $\alpha_4 = 16$.

α_3	0.025	0.05	0.1	0.2
Bit Acc (%)	99	99	99	99
Message Acc (%)	73	71	94	94

Table 5. Study on LSE loss’s coefficient α_3

α_4	10	12	14	16
PSNR	33.16	33.18	33.30	32.73
Bit Acc (%)	99	99	99	99
Message Acc (%)	94	97	96	99
# Iterations to pass τ_1	41K	34K	31K	29K

Table 6. Study on message coefficient α_4 .

5. Discussion

Limitations: Even with its strength against color intensity shifts, our approach faces a challenge: geometric transformations like rotation or perspective warp. Unlike color alterations, these transformations can disrupt the spatial relationships in the image, jeopardizing the integrity of the encoded message’s hidden pattern within steganographic images. Future research could focus on developing adaptive techniques that maintain the encoded message’s integrity despite geometric distortions.

Conclusion: In conclusion, we have made three key contributions. First, we have introduced a novel metric of message accuracy, emphasizing precise alignment between the extracted hidden message and the originally embedded message. Second, we have devised a novel LSE loss to significantly enhance the entire message recovery, meeting the strict requirements of the message accuracy metric. Next, we have proposed our approach Stable Messenger with the latent-content-aware message encoding technique leveraging a pretrained SD, contributing to a better trade-off between image quality and message recovery. Most importantly, our approach can work in both cover and generative modes, where the latter is very crucial for protecting and verifying generated photo-realistic images from very powerful text-to-image generative models.

References

- [1] Midjourney. <https://www.midjourney.com>. 1
- [2] Stable Diffusion. <https://github.com/Stability-AI/stablediffusion>. 1
- [3] Shahzad Alam, Vipin Kumar, Waseem A Siddiqui, and Musheer Ahmad. Key dependent image steganography using edge detection. In *2014 Fourth International Conference on Advanced Computing & Communication Technologies*, pages 85–88. IEEE, 2014. 1
- [4] Yogesh Balaji, Seungjun Nah, Xun Huang, Arash Vahdat, Jiaming Song, Qinsheng Zhang, Karsten Kreis, Miika Aittala, Timo Aila, Samuli Laine, Bryan Catanzaro, Tero Karras, and Ming-Yu Liu. ediff-i: Text-to-image diffusion models with an ensemble of expert denoisers. *ArXiv*, abs/2211.01324, 2022. 1
- [5] Tu Bui, Shruti Agarwal, Ning Yu, and John Collomosse. Rosteals: Robust steganography using autoencoder latent space. In *Proceedings of the IEEE/CVF Conference on Computer Vision and Pattern Recognition*, pages 933–942, 2023. 2, 3, 4, 5, 6, 8
- [6] Ching-Chun Chang. Neural reversible steganography with long short-term memory. *Security and Communication Networks*, 2021:1–14, 2021. 2
- [7] Huiwen Chang, Han Zhang, Jarred Barber, AJ Maschinot, José Lezama, Lu Jiang, Ming Yang, Kevin P. Murphy, William T. Freeman, Michael Rubinstein, Yuanzhen Li, and Dilip Krishnan. Muse: Text-to-image generation via masked generative transformers. *ArXiv*, abs/2301.00704, 2023. 1
- [8] Xintao Duan, Kai Jia, Baoxia Li, Daidou Guo, En Zhang, and Chuan Qin. Reversible image steganography scheme based on a u-net structure. *IEEE Access*, 7:9314–9323, 2019. 2
- [9] Patrick Esser, Robin Rombach, and Bjorn Ommer. Taming transformers for high-resolution image synthesis. In *Proceedings of the IEEE/CVF conference on computer vision and pattern recognition*, pages 12873–12883, 2021. 6
- [10] Pierre Fernandez, Guillaume Couairon, Hervé Jégou, Matthijs Douze, and Teddy Furon. The stable signature: Rooting watermarks in latent diffusion models. *arXiv preprint arXiv:2303.15435*, 2023. 2, 3
- [11] Kazem Ghazanfari, Shahrokh Ghaemmaghami, and Saeed R Khosravi. Lsb++: An improvement to lsb+ steganography. In *TENCON 2011-2011 IEEE Region 10 Conference*, pages 364–368. IEEE, 2011. 2
- [12] Micah Hodosh, Peter Young, and Julia Hockenmaier. Framing image description as a ranking task: Data, models and evaluation metrics. *Journal of Artificial Intelligence Research*, 47:853–899, 2013. 5
- [13] Vojtvech Holub and Jessica Fridrich. Designing steganographic distortion using directional filters. In *2012 IEEE International workshop on information forensics and security (WIFS)*, pages 234–239. IEEE, 2012. 2
- [14] Vojtvech Holub, Jessica Fridrich, and Tomávs Denmark. Universal distortion function for steganography in an arbitrary domain. *EURASIP Journal on Information Security*, 2014:1–13, 2014. 2
- [15] Chen-Hsiu Huang and Ja-Ling Wu. Image data hiding with multi-scale autoencoder network. *arXiv preprint arXiv:2201.06038*, 2022. 2
- [16] Mark J Huiskes and Michael S Lew. The mir flickr retrieval evaluation. In *Proceedings of the 1st ACM international conference on Multimedia information retrieval*, pages 39–43, 2008. 2, 5, 6, 8
- [17] Tero Karras, Miika Aittala, Janne Hellsten, Samuli Laine, Jaakko Lehtinen, and Timo Aila. Training generative adversarial networks with limited data. *Advances in neural information processing systems*, 33:12104–12114, 2020. 2, 5, 6
- [18] Changhoon Kim, Kyle Min, Maitreya Patel, Sheng Cheng, and Yezhou Yang. Wouaf: Weight modulation for user attribution and fingerprinting in text-to-image diffusion models. *arXiv preprint arXiv:2306.04744*, 2023. 2
- [19] Jari Korhonen and Junyong You. Peak signal-to-noise ratio revisited: Is simple beautiful? In *2012 Fourth International Workshop on Quality of Multimedia Experience*, pages 37–38. IEEE, 2012. 5
- [20] Xiaoxia Li and Jianjun Wang. A steganographic method based upon jpeg and particle swarm optimization algorithm. *Information Sciences*, 177(15):3099–3109, 2007. 2
- [21] Weiqi Luo, Fangjun Huang, and Jiwu Huang. Edge adaptive image steganography based on lsb matching revisited. *IEEE Transactions on information forensics and security*, 5(2):201–214, 2010. 1
- [22] Yihan Ma, Zhengyu Zhao, Xinlei He, Zheng Li, Michael Backes, and Yang Zhang. Generative watermarking against unauthorized subject-driven image synthesis. *arXiv preprint arXiv:2306.07754*, 2023. 2
- [23] Daniele Mari and Simone Milani. Features denoising for learned image coding. In *2022 10th European Workshop on Visual Information Processing (EUVIP)*, pages 1–6. IEEE, 2022. 2, 5, 6
- [24] Ruohan Meng, Steven G Rice, Jin Wang, and Xingming Sun. A fusion steganographic algorithm based on faster r-cnn. *Computers, Materials & Continua*, 55(1), 2018. 2
- [25] Jarno Mielikainen. Lsb matching revisited. *IEEE signal processing letters*, 13(5):285–287, 2006. 1
- [26] KA Navas, Mathews Cheriyan Ajay, M Lekshmi, Tampy S Archana, and M Sasikumar. Dwt-dct-svd based watermarking. In *2008 3rd International Conference on Communication Systems Software and Middleware and Workshops (COMSWARE'08)*, pages 271–274. IEEE, 2008. 2
- [27] Bui Cong Nguyen, Sang Moon Yoon, and Heung-Kyu Lee. Multi bit plane image steganography. In *Digital Watermarking: 5th International Workshop, IWDW 2006, Jeju Island, Korea, November 8-10, 2006. Proceedings 5*, pages 61–70. Springer, 2006. 1
- [28] Alex Nichol, Prafulla Dhariwal, Aditya Ramesh, Pranav Shyam, Pamela Mishkin, Bob McGrew, Ilya Sutskever, and Mark Chen. Glide: Towards photorealistic image generation and editing with text-guided diffusion models. In *International Conference on Machine Learning*, 2021. 1
- [29] Tomávs Pevný, Tomávs Filler, and Patrick Bas. Using high-dimensional image models to perform highly undetectable steganography. In *Information Hiding: 12th International*

- Conference, IH 2010, Calgary, AB, Canada, June 28-30, 2010, Revised Selected Papers 12*, pages 161–177. Springer, 2010. [2](#)
- [30] Niels Provos. Defending against statistical steganalysis. In *10th USENIX Security Symposium (USENIX Security 01)*, 2001. [2](#)
- [31] Aditya Ramesh, Prafulla Dhariwal, Alex Nichol, Casey Chu, and Mark Chen. Hierarchical text-conditional image generation with clip latents. *ArXiv*, abs/2204.06125, 2022. [1](#)
- [32] Robin Rombach, Andreas Blattmann, Dominik Lorenz, Patrick Esser, and Björn Ommer. High-resolution image synthesis with latent diffusion models. In *Proceedings of the IEEE/CVF conference on computer vision and pattern recognition*, pages 10684–10695, 2022. [2](#), [4](#), [5](#)
- [33] Chitwan Saharia, William Chan, Saurabh Saxena, Lala Li, Jay Whang, Emily L Denton, Kamyar Ghasemipour, Raphael Gontijo Lopes, Burcu Karagol Ayan, Tim Salimans, et al. Photorealistic text-to-image diffusion models with deep language understanding. *Advances in Neural Information Processing Systems*, 35:36479–36494, 2022. [1](#)
- [34] Mustafa Sabah Taha, Mohd Shafry Mohd Rahem, Mohammed Mahdi Hashim, and Hiyam N Khalid. High payload image steganography scheme with minimum distortion based on distinction grade value method. *Multimedia Tools and Applications*, 81(18):25913–25946, 2022. [2](#)
- [35] Matthew Tancik, Ben Mildenhall, and Ren Ng. Stegastamp: Invisible hyperlinks in physical photographs. In *Proceedings of the IEEE/CVF conference on computer vision and pattern recognition*, pages 2117–2126, 2020. [1](#), [2](#), [3](#), [5](#), [6](#), [8](#)
- [36] Zhou Wang, Alan C Bovik, Hamid R Sheikh, and Eero P Simoncelli. Image quality assessment: from error visibility to structural similarity. *IEEE transactions on image processing*, 13(4):600–612, 2004. [5](#)
- [37] Raymond B. Wolfgang and Edward J. Delp. A watermark for digital images. *Proceedings of 3rd IEEE International Conference on Image Processing*, 3:219–222 vol.3, 1996. [2](#)
- [38] KA Zhang, L Xu, A Cuesta-Infante, and K Veeramachani. Robust invisible video watermarking with attention. arxiv 2019. *arXiv preprint arXiv:1909.01285*. [1](#), [2](#), [3](#)
- [39] Richard Zhang, Phillip Isola, Alexei A Efros, Eli Shechtman, and Oliver Wang. The unreasonable effectiveness of deep features as a perceptual metric. In *Proceedings of the IEEE conference on computer vision and pattern recognition*, pages 586–595, 2018. [5](#)
- [40] Xinpeng Zhang and Shuozhong Wang. Steganography using multiple-base notational system and human vision sensitivity. *IEEE signal processing letters*, 12(1):67–70, 2004. [1](#)
- [41] Jiren Zhu, Russell Kaplan, Justin Johnson, and Li Fei-Fei. Hidden: Hiding data with deep networks. In *Proceedings of the European conference on computer vision (ECCV)*, pages 657–672, 2018. [1](#), [2](#), [3](#)